Catalytic hydrogenolysis of lignin

Wang, Zhiwen; Deuss, Peter

Published in:
Chemsuschem

DOI:
10.1002/cssc.202101527

Publication date:
2021

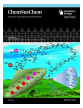

Catalytic Hydrogenolysis of Lignin: The Influence of Minor Units and Saccharides

Zhiwen Wang[a] and Peter J. Deuss*[a]

The precise elucidation of native lignin structures plays a vital role for the development of "lignin first" strategies such as reductive catalytic fractionation. The structure of lignin and composition of the starting material has a major impact on the product yield and distribution. Here, the differences in structure of lignin from birch, pine, reed, and walnut shell were investigated by combining detailed analysis of the whole cell wall material, residual enzyme lignin, and milled wood lignin. The results of the 2D heteronuclear single quantum coherence NMR analysis could be correlated to the product from Ru/C-catalyzed hydrogenolysis if monomeric products from ferulate and *p*-coumaryl and its analogous units were also appropriately considered. Notably, residual polysaccharide constituents seemed to influence the selectivity towards hydroxy-containing monomers. The results reinforced the importance of adequate structural characterization and compositional analysis of the starting materials as well as distinct (dis)advantages of specific types of structural characterization and isolation methods for guiding valorization potential of different biomass feedstocks.

Introduction

With the inevitable limits to the consumption of fossil fuels, lignocellulosic biomass is the most promising feedstock for development of a sustainable chemical and fuel supply.[1,2] Among the main building blocks of biomass, lignin is the only polymer that nearly exclusively consists of aromatic units, and considerable attention has gone into achieving high-value products from lignin.[3] Polymeric lignin is constructed mainly from three monolignols known as *p*-coumaryl alcohol (H), coniferyl alcohol (G), and sinapyl alcohol (S) that are biosynthesized from phenylalanine (Phe) (Figure 1a)[4] and subsequently undergo radical coupling (Figure 1b),[5] favoring the formation of the aryl ether (β-O-4) linkage among other linkages such as resinols (β-β) and phenylcoumaran (β-5) (Figure 1c).[6–9]

H, ferulate (FA), and *p*-coumarate (*p*CA) units are less abundant units, but their presence can have a significant impact on the lignin structure.[10] For example, the lower unpaired electron density on the phenolic oxygen gives *p*-coumaryl alcohol the highest possibility to serve as a starting site for lignin polymerization, which means an increasing amount of H units (yellow in Figure 1a,c) can lead to overall lower-molecular-weight lignin.[11] Additionally, such minor units such as FA (blue in Figure 1a,c) and *p*CA (red in Figure 1a,c), often found in herbaceous biomasses, can serve as terminal groups and pendent chains, which make the quantification and elucidation of H units of lignin a challenge.[12] FA and *p*CA have also been claimed to serve as constituents of hemicellulose (or as bridging unit between lignin and hemicellulose, Figure 1c).[13] These non-homologous building blocks and complex linkages increase the challenge of refining and structural elucidation and the valorization of lignin, thus understanding their influence is pivotal for maximization of biomass utilization.[3,14–17]

Several promising lignin conversion technologies have been studied such as pyrolysis, hydrotreatment and selective oxidation of hydroxyls for modification and degradation.[18–22] Among these, reductive catalytic fractionation (RCF) or catalytic hydrogenolysis of isolated lignin have been intensively studied as a lignin-first bio-refinery strategy with the potential to produce valuable alkyl phenolic monomers from lignin.[23] Various catalytic systems with metal-based catalysts have been explored to produce functional aromatic monomers from different biomasses, and the product portfolio was shown to be tunable by the choice of catalyst and reaction conditions.[24–26] The monomers can be converted to marketable added-value chemicals by catalytic funneling.[22,27] These monomers are mainly obtained by the cleavage of the β-O-4 linkage and thus monomer yields closely correlate with the structure and composition of the staring material.[21] Studies have shown that the structure and quality of lignin are significantly important for the lignin-first oriented RCF or the hydrogenolysis of isolated lignins and are easily influenced by lignocellulosic species and extraction or isolation methods.[3,28,29] Therefore, prior to reductive fractionation, a robust and comprehensive method for analyzing the main structure of lignin to guide valorization potential is desired.

Many approaches have been applied to analyze the structure of lignin such as thioacidolysis (TA), pyrolysis, nitrobenzene oxidation, and derivatization followed by reductive cleavage (DFRC), all in combination with GC-MS, as well as carbon-13 cross-polarization/magic angle spinning (CP/MAS)

[a] Z. Wang, Dr. P. J. Deuss
Department of Chemical Engineering (ENTEG),
University of Groningen
Nijenborgh 4, 9747 AG Groningen (The Netherlands)
E-mail: p.j.deuss@rug.nl

Supporting information for this article is available on the WWW under https://doi.org/10.1002/cssc.202101527

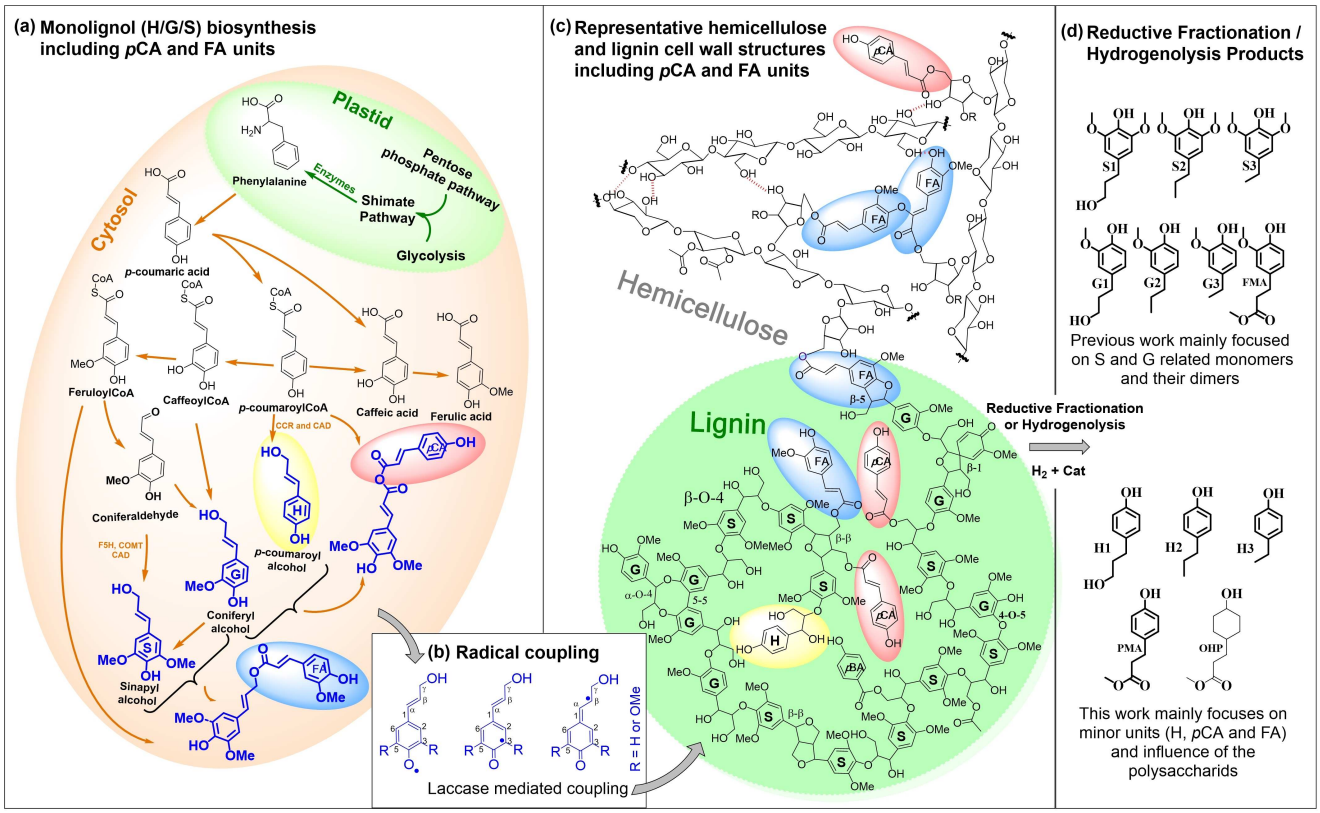

Figure 1. Overview of the fate of aromatic components in biomass upon reductive fractionation or hydrogenolysis with specific focus on H, *p*CA, and FA units. (a) Simplified monolignol biosynthesis pathways. (b) Radical species formed upon enzymatic oxidation of the monolignols. (c) Representative structures of lignin and hemicellulose in the cell wall highlighting minor units. (d) Monomer products released from reductive fractionation or hydrogenolysis.

solid-state NMR (CPMAS SS NMR) and infrared (IR) spectroscopy.[30–37] Proportions of units of the original lignin can roughly be estimated by quantification of the different monomers from reductive hydrogenolysis and vice versa as well as for the identification of difficult linkages such as the 4-O-5.[36,38] Precise analysis of lignin by extrapolating degraded fragments needs careful consideration of products derived from units originally connected by C–C bond in the lignin.[37]

Currently, there is still limited knowledge on influence of minor units on the product distribution from lignin hydrogenolysis, although this is important for biomass sources with significant quantities of these, such as walnut shell and reed. This is hampered by challenges in their accurate quantification due to overestimation.[10] Therefore, a good biomass analysis protocol that can deal with such challenges can give improved insight in the highly desired prediction of the expected product portfolio from specific biomass sources.

Multi-dimensional NMR techniques such as heteronuclear single quantum coherence (HSQC) can provide detailed structural information.[40–42] Whole-cell-wall (WCW) gel-state NMR spectroscopy can be used to directly analyze the lignin in plant cells but yields very complex spectra.[10] Alternatively, mild enzymatic hydrolysis can achieve removal of a majority of polysaccharides providing isolated residual enzyme lignin (REL), although intensive ball milling treatment has to be applied to enhance the enzyme activity.[43] Furthermore, signals from residual proteins introduced by the enzyme treatment can overlap with those of H units in lignin, which restricts estimation of the H content.[44] Mildly extracted milled wood lignin (MWL) gives cleaner well-solvated lignin fragments for 2D HSQC NMR analysis, which can partly represent the larger lignin polymeric structure.[43,45–47]

In this study we aim to get insight in the value of different sample preparation techniques and analysis methods to correlate to lignin hydrogenolysis product mixtures with emphasis on the minor units. For this purpose, four representative biomasses were selected for the WCW analysis, REL isolation, and MWL extraction, and the results were correlated to obtained Ru/C RCF product mixtures. The lignin substrate samples were subjected to a detailed 2D HSQC NMR study complemented with Fourier-transform (FT)IR spectroscopy, scanning electron microscopy (SEM), thermal gravimetric analysis and first-derivative thermogravimetric (TGA/DTG), and gel permeation chromatography (GPC) analyses. Product mixture correlation was further extended to catalytic hydrogenolysis of isolated lignins samples. The difference in the lignin structures in the different biomass samples and those of REL and MWL were comprehensively analyzed in order to understand which lignin analysis protocol can provide what insight on the expected hydrogenolysis product mixtures, in particular for elucidation of the minor H units and its analogous units in

terms of overestimation, monomer origin, and influence of the presence of polysaccharides in the substrate.

Results and Discussion

The structure of lignin is inevitably altered during the isolation or extraction process, which hampers the establishment of adequate correlations between the native lignin structure and the products obtained from lignin-first methods such as RCF. Therefore, several methods that are known to give insight into the structure of native-like lignin are combined in this study. Firstly, a gel-state 2D HSQC NMR spectrum was collected in order to illustrate the as-close-to-native structure of lignin in the cell wall material. This was done by directly swelling the ball milled WCW material in DMSO-d_6/pyridine-d_5 (4:1, *v*/*v*). Secondly, REL was isolated by milder enzymatic hydrolysis of polysaccharides via double round sequential treatment using optimized parameters from our previous publication.[49] Thirdly, MWL was isolated by multiple neutral 1,4-dioxane extractions. The REL and MWL samples served as typical isolated native-like lignins and were used for the comparison to investigate the difference in structural information that could be obtained and the limitation to each of these analysis procedures.

The unit constituents of lignin depend on the biomass species. Guaiacyl (G) units and minor amounts of *p*-hydroxyphenyl (H) units typically comprise gymnosperms lignins, whereas angiosperm dicot lignin consists of syringyl (S) and G units with even lower amounts of H units. As mentioned in the introduction walnut shells contain a particularly high amount of H units, and grasses typically have high amounts of H derivatives such as *p*CA. Therefore, the selection of different biomass species is significant for the outcome of lignin-first methodologies, and several significantly different biomass samples were selected to represent hardwood, softwood, grass, and nutshell lignocellulosic biomass. Birch wood was selected to represent a hardwood, as used in some current biorefineries.[21,22] Pine wood was selected as the most universal gymnosperm and used to represent a typical softwood. Reed, a fast-growing and widely distributed grass, was used here as a typical grassy lignocellulose sample. As walnut shell contains a relatively high amount of lignin and more than 5.5 megatons walnuts (with shells) were produced in 2016,[51] it was set as a non-wood material to study lignin that is not a specific hard- or softwood. After successfully obtaining these samples, analysis of the yield, carbohydrate analysis, thermal stability, and molecular distribution was conducted. (see S2.1, S2.3, S2.4, and S2.6 in the Supporting Information) before turning to analysis by 2D HSQC NMR spectroscopy.

Qualitative 2D HSQC NMR analysis

As far as we are aware, walnut shell and reed gel-state 2D HSQC NMR spectra have not been previously reported. Therefore, we aimed to find the parameters for optimal formation of a gel sample for NMR spectroscopy in DMSO-d_6/pyridine-d_5. This was achieved for walnut shell, which is the hardest of the four materials, by a time course of ball milling time over 24 h and with around 4 h sonication (detailed study see S2.2). The 2D HSQC NMR spectra of all the four WCW gel-state samples were collected under the same optimized conditions (Figure 2). Although the signals of the 2D HSQC NMR from WCW samples showed complexity and overlap, most signals from linkages and aromatic rings of lignin could be well distinguished after careful analysis, which showed valuable information about the saccharide and lignin structures (see Table S2 for assignments).[10,48,52,53]

Looking at the aromatic region (AR, Figure 2), WCW_Birch showed predominantly S signals, and the signal of α-ketone structures of S units was relatively strong compared to the other samples. G unit signals dominated the spectrum of the WCW_Pine, while the intensity of G was similar to S units for walnut shell and reed. As expected, a considerable strong H signal only appeared on the spectrum of WCW_Walnut. Both *p*-coumarate (*p*CA) and ferulate (FA) were clearly more abundant in WCW_Reed when compared to the other biomasses. Signals from polysaccharides crowded in the (oxygenated) aliphatic region (AL, Figure 2), which overlapped with the signals of the linkage motifs of lignin, such as the overlap between β-O-4$_\alpha$ and 2,3-di-O-AC-β-D-Xyl*p*, as well as γ position of β-O-4 and β-5 with C-I$_6$ and X-I$_5$, which increased the challenge for assigning the signals of lignin and relative comparison by directly using WCW 2D HSQC NMR specta (detailed discussion see S2.5 in the Supporting Information).[10]

A lot of signals could still be assigned by using the available literature; nevertheless, 2D HSQC NMR analysis of REL samples can be significantly easier due to clearer signals and less overlap. This can be observed in Figure 3, where many more signals could be assigned with increased confidence, in particular the (oxygenated) aliphatic region (AL, Figure 3) due to reduced interference of carbohydrate signals. A definite signal of acylated aryl ethers (β-O-4′) resulting from the acylation of aryl ethers (β-O-4) via *p*CA or FA appeared in REL_Reed.[54] This is a possible bridge for connecting lignin and saccharides, in line with the discussion of high amount of saccharide impurities and *p*CA and FA in REL_Reed. In addition, signals for tricin, one member of the flavonoid family found in some grass biomasses, were now clearly observed in the aromatic region (AR, Figure 3) of REL_Reed.[8] For all samples the different signals in the aromatic units for H-type units and derivatives became more clearly visible in the REL spectra. The exception is the H$_{2,6}$ signal in REL_Walnut, which was similar but less intense compared to that of WCW. The H units content rarely reaches more than 5% except for some genetically modified plants;[55] however, our analysis indeed showed that walnut shell contains an unusually high content of H units (see below) making it still clearly visible in the WCW samples. Dibenzodioxocin (D) units, from coupling between a monolignol and biphenyl unit, in REL_Birch showed the weakest signal among all the four REL samples, as the biphenyl units are solely formed from coupling of G or H units. REL_Pine displayed a similar type of G lignin to that of WCW_Pine, except some signals from end groups. For instance, the cinnamyl alcohol end group (X1) and the cinnamaldehyde end group (X2) were

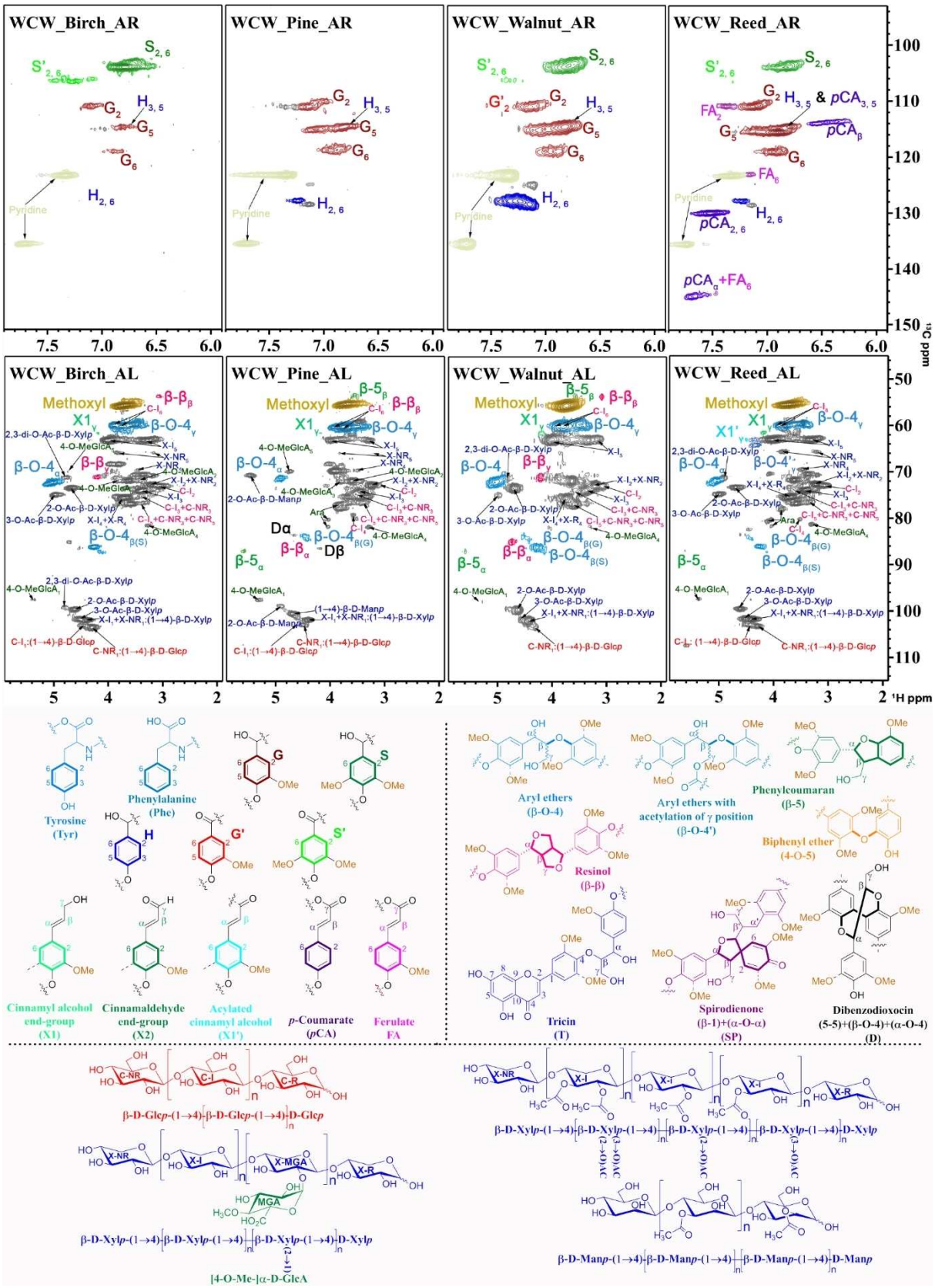

Figure 2. 2D HSQC NMR spectra of the WCW from the four biomasses (DMSO-d_6/pyridine-d_5, 4:1, *v/v*). AR: aromatic region; AL: aliphatic region. The most common polysaccharide and lignin label system is used. The structure and corresponding signals in the spectra were color-coded with each other.

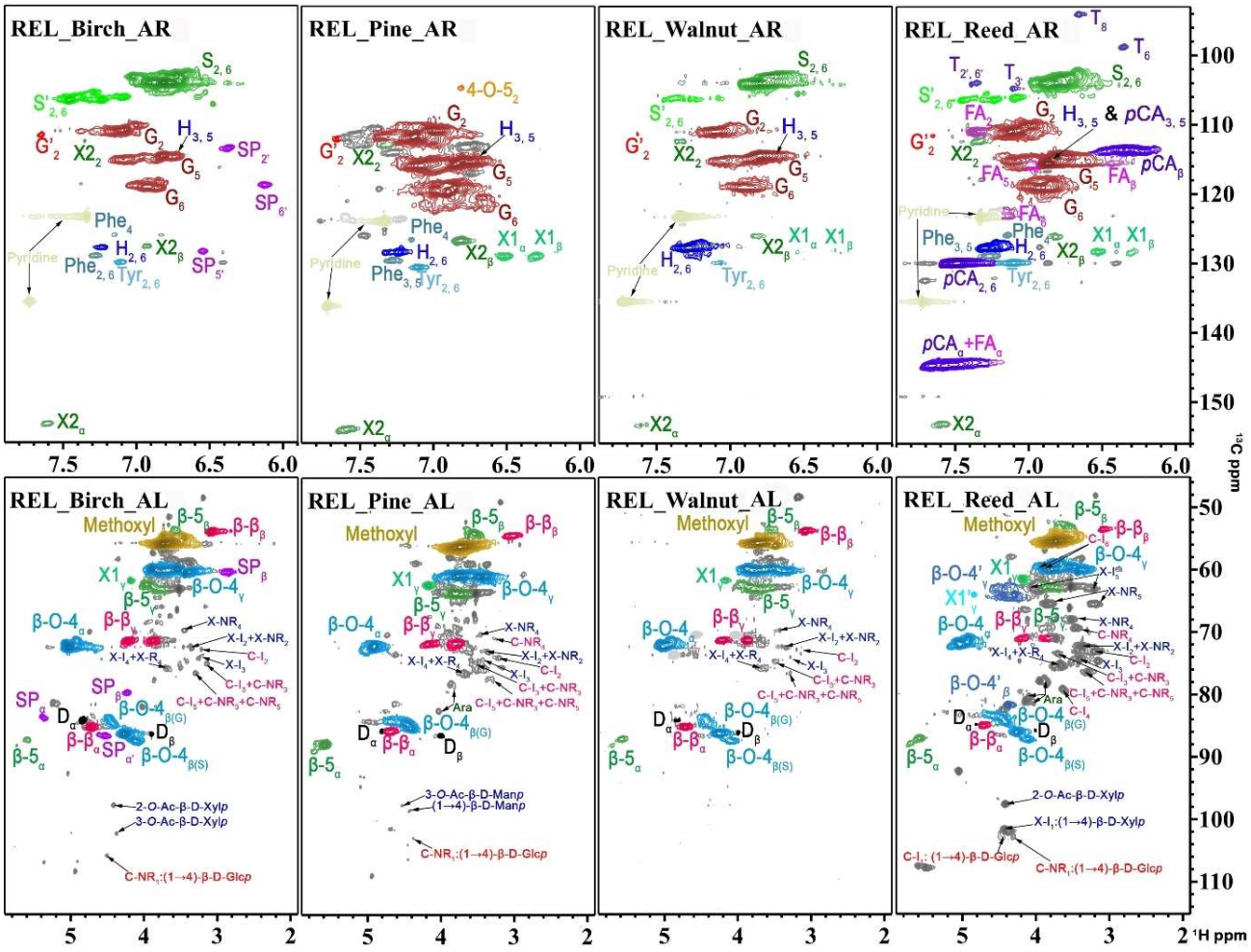

Figure 3. 2D HSQC NMR spectra of REL isolated from the four biomasses (DMSO-d_6/pyridine-d_5, 4:1, *v/v*). The most common polysaccharide and lignin label system is used. The structures to the corresponding signals in the spectra were shown in Figure 2.

clearly visible. The units of D and 4-O-5 are normally present in low levels and hard to be detected,[56] but evident cluster signals of D and 4-O-5 were observed in REL_Pine around 83.97/4.99 ppm (D_α), 86.35/4.01 ppm (D_β), and 104.80/6.81 ppm (4-O-5_2), respectively. These two minor units are traditionally thought of as cross-linking sites in lignin but have recently been considered as end groups of lignin with phenolic groups.[56,57] A clear disadvantage of the 2D HSQC NMR analysis of REL samples is that the aromatic region (AR) of all the spectra was contaminated by signals from protein residues, such as Phe and Tyr originating from the enzyme cocktail used for the carbohydrate removal and possibly also from residual protein left behind from the biomass substrate.

MWL can alleviate the contaminations originating from carbohydrates and residual proteins, giving cleaner spectra (Figure 4), but at the expense of some signals for minor linkages. For instance, no clear signals of 4-O-5 and end group were observed for MWL_Pine in contrast to the corresponding REL spectrum. A well-isolated signal of H units appeared, which was also here strongest for MWL_Walnut compared to MWL from other biomasses. The spectra of MWL_Reed showed similar aromatic signals as those found in WCW_Reed and REL_Reed. Clearer signals for tricin were found in the MWL_Reed spectrum, which is likely because tricin is involved in initializing a polymer chain, and thus acts as an end group.[8] Such end groups are enriched due to the 1,4-dioxane extraction as part of the MWL procedure that favors extraction of shorter oligomeric chains that are more soluble. The molecular weight (M_W) distribution of MWLs and RELs clearly revealed that RELs have a high molecular weight (Figure S18) with weight-average molecular weight much higher than that of their corresponding MWL samples (Table S4), showing that indeed MWL just contains shorter oligomers released from the pendent part of lignin or cleaved from the high-molecular part of lignin during ball milling. Moreover, for REL spectra of these four biomasses, stronger H units are observed for lignin with lower M_W. For instance, the M_W sequence of RELs followed REL_Walnut < REL_Reed < REL_Pine < REL_Birch, while the relative intensity of the signals from H in the 2D HSQC NMR spectra followed a sequence of REL_Walnut > REL_Reed > REL_Pine > REL_Birch (detailed discussion see S2.6). It seemed that the MW was associated with the percentage of H unit in lignin, which might

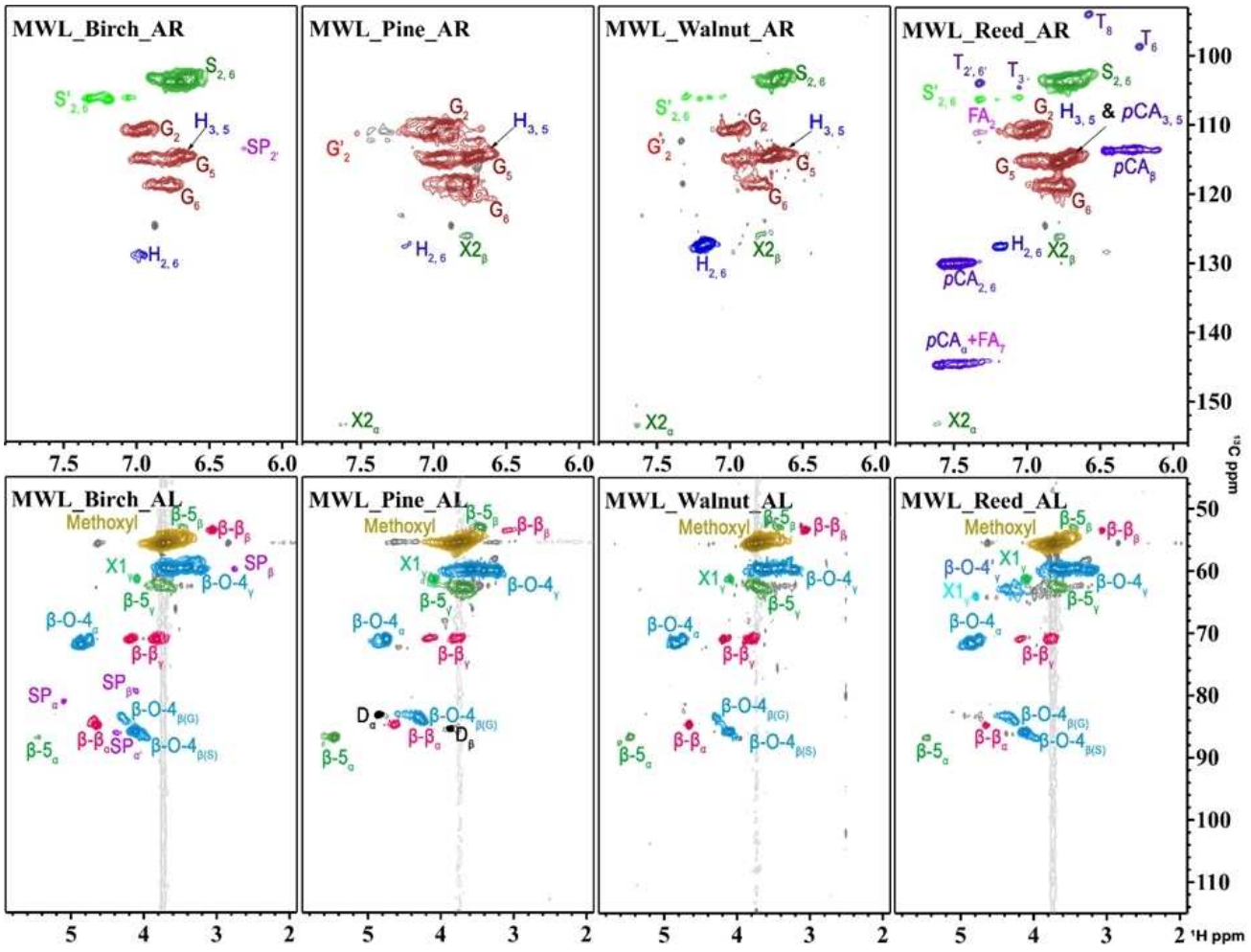

Figure 4. 2D HSQC NMR spectra of MWL isolated from the four biomasses (DMSO-d_6). The most common polysaccharide and lignin label system is used. The structures to corresponding signals in the spectra were shown in Figure 2.

be due to H units having a tendency to serve as starting sites during lignin biosynthesis.[11]

Overall, qualitative analysis of WCW samples not only clearly revealed the main signals of aromatic rings of lignin but also was a great way to study the saccharide part of the biomasses, but had limitations on revealing minor linking motifs and minor aromatic units of lignin. REL could well avoid the limitations of WCW analysis. However, the protein contamination seriously influenced the estimation of the H units fin REL samples. MWL isolation could overcome these adverse effects of these contaminations but led to overrepresentation of signals from end groups due to MWL consisting of shorter extracted lignin chains.

Semi-quantification of 2D HSQC NMR spectra

It is a challenge to absolutely quantify the linkages and pendant units of lignin by 2D HSQC NMR spectra, as signal integrations can be influenced by many parameters, such as T_1 and T_2 relaxation rates, carbon pulse offset effects, and multiplicity and magnitude of coupling constants.[58] Pendant units, such as H units, *p*-hydroxybenzoates (*p*B), and *p*CA can be easily overestimated as the difference of relaxation time between the interior structure of lignin and these terminal groups. Nevertheless, semi-quantification of the spectra based on signals that represent C9 units still provides valuable information such as relative reliable S/G ratios and relative amounts of the main linking units of lignin from similar resources.

To demonstrate the difference in information that can be extracted from these different types of lignin analyses, semi-quantitative analysis was performed by signal integrations (Table 1). The semi-quantification revealed that structural information of lignin extracted from WCW_Reed, REL_Reed, and MWL_Reed had the highest concordance among the four biomasses (apart from FA quantities, see discussion below), while for the other biomasses some differences could clearly be observed between the differently prepared lignin NMR samples. Examples are the unusual proportion of H units in walnut shell samples and variation of S/G ratio for birch samples as well as quite big difference of the β-O-4 linkage quantification for the pine samples.

Table 1. Composition of the lignin aromatic units, S/G ratio, and relative abundance of main inter-unit linkages of WCW, MWL, and REL.

Sample	S[a] [%]	S′[a] [%]	G[a] [%]	G′[a] [%]	H[a] [%]	FA[c] [%]	*p*CA[c] [%]	β-O-4[a] [%]	β-5[a] [%]	β-β[a] [%]	S/G[a]
WCW_Birch	65	13	22	<1	1	<1	<1	57	1	3	3.5
REL_Birch	68	9	22	1	1[b]	<1	<1	58	3	8	3.4
MWL_Birch	57	8	32	1	3	<1	<1	53	4	11	2.0
WCW_Pine	0	0	91	2	7	<1	<1	34	11	2	–
REL_Pine	0	0	93	5	2[b]	<1	<1	40	17	6	–
MWL_Pine	0	0	94	4	2	<1	<1	34	17	6	–
WCW_Reed	35	3	56	0	6	12	24	49	9	1	0.7
REL_Reed	40	3	52	0	6[b]	7.5	23	48	8	4	0.8
MWL_Reed	41	3	53	0	3	3	20	45	9	4	0.8
WCW_Walnut	38	6	32	<1	24	<1	<1	47	9	8	1.3
REL_Walnut	50	4	34	1	11[b]	<1	<1	50	7	10	1.6
MWL_Walnut	39	5	40	2	15	<1	<1	48	13	10	1.1

[a] S = syringyl units; S′ = syringyl with a α-ketone structure; G = guaiacyl structure; G′ = guaiacyl units with a α-ketone structure; H = *p*-hydroxylphenyl units; FA = ferulate; *p*CA = *p*coumarate; β-O-4 = aryl ether linkage; β-β = resinols; β-5 = phenylcoumaran. The data was calculated by semi-quantitative method and based on the total amount of C9 units, and the molar percentage was based on the integration of the signal at α position of the linkage divided by the total integration of S (1/2 $S_{2,6}$), S′ (1/2 $S'_{2,6}$), G (G_2), G′(G'_2), H (1/2 $H_{2,6}$), S/G ratio obtained by (1/2 $S_{2,6}$ + 1/2 $S'_{2,6}$)/(G_2 + G'_2) (see Figure 2 for structures). [b] As REL samples were contaminated with proteins and the signals of $H_{2'6}$ units were overlapped with phenylalanine from residue protein, the integration of H units was based on the overlapped signals. The integration values for the H units might be slightly larger than their actual H units because of the overlap of $Phe_{3,5}$, in particular for Birch_REL and Pine_REL. [c] FA (FA_2) and *p*CA (1/2 $pCA_{2,6}$) were calculated by C9 units (see [a]).

Roughly, S/G ratios of WCW and REL were higher than that of MWL, which is explained as S units are harder to be released from biomass in organic extraction of lignin as S units always present in the main back bone of the lignin and high steric hindrance.[59] In addition, higher proportions of H units were found in WCW compared to that of corresponding REL and MWL samples, confirming overestimation of H units by the method of gel-state WCW.[10] Higher levels (>10%) H units, with a relatively lower percentage of G units, were determined in WCW, REL, and MWL of walnut shell, indicating that walnut shell-derived lignin indeed contains a higher proportion of H units. This unusually high H content was observed before in specifically extracted walnut shell lignin that was shown to contain nearly 30% H units.[60] The discrepancy for the lignins was also found for the semi-quantification of *p*CA and FA for reed samples. The percentage of *p*CA was similar among WCW, REL, and MWL from reed, while FA in WCW_Reed was much higher than the corresponding lignins. This is likely because FA is part of the hemicellulose structure and actually might only be part of the lignin as bridge between lignin and hemicellulose. *p*CA incorporates in lignin as a pendant or end group.[61] Therefore, FA could be removed during the enzyme treatment and hardly extracted as it connected with saccharide, and *p*CA was easily released together with lignin during organic extraction and conserved during enzyme treatment.

All the samples obtained by different protocols revealed a similar proportion of β-O-4 linkages. As expected, birch with a higher S content showed the highest amount of β-O-4 linkages among all the WCW samples. By contrast, the abundance of β-O-4 linkages in WCW_Pine was determined as the lowest, as it only contains G units with minor H units. In general, the sequence of β-O-4 followed the order of birch > reed > pine, which is consistent with order of the percentage of S units. This observation was also found in semi-quantification of REL and MWL for these three biomasses. However, in the case of walnut shell, some abnormalities were observed. For instance, in contrast to the reed samples, the data of WCW and MWL from walnut shell have higher level of S units, but it did not result in a higher content of β-O-4. This may be due to the unusually high amount of H units that have a stronger tendency to form other linkages such as 5–5 linkages; this can also be confirmed by comparing the intensity of dimers for reed and walnut shell samples from reductive hydrogenolysis (see the Supporting Information S3, Figure S24-27 and Table S7, and discussion below). Relatively high amounts of β-5 and β-β linkages were found in MWL compared to their corresponding WCW and REL samples for all the four biomasses, which showed the limitation of MWL to represent native constituents of lignin. These are relatively stable structures having a higher possibility to be well conserved during extraction and also might be further enriched as they occur more in shorter extractable lignin chains. The influence of higher proportion of S units was also shown in the abundance of β-5 linkages, but the order followed the opposite trend as S units cannot form β-5 linkages. However, walnut shell contained a much lower content of G units than that of reed, but β-5 linkage content was similar for the two biomasses and lower than that of lignin from pine. Also, this might be because walnut shell contained a higher amount of H units and the *p*-coumaryl alcohol favoring the production of C–C linkages.[62] For instance, the amount of β-5 linkages of MWL_Walnut (13%) was far more than that of corresponding REL (7%), supporting our view that the higher amount of H units leads to more stable C–C linkages such as the β-5 linkages more easily extracted by organic extraction. Samples from reed contained the lowest amount of β-β linkages among the four biomass samples, which might be due to the fact that a certain amount of γ-hydroxy groups of the β-O-4 units was acetylated as revealed by the evident signals of the acylated units (β-O-4′$_\gamma$) in the spectra. This is the result of an acylated precursor in the biosynthesis (Figure 1a),[63,64] which also decreases the possibility for them to radically couple to form a β-β linkage.[65] Therefore, lignin fragments with higher percentage of β-O-4′$_\gamma$ can indeed be

expected to also contain a relatively lower content of β-β linkages, as is indeed observed when comparing the ratio of β-O-4$_\gamma$ and β-O-4′$_\gamma$ of WCW_Reed, REL_Reed, and MWL_Reed (9.7, 5.2, and 5.6, respectively, based on C9 units) with the β-β linkages in these samples.

Reductive catalytic fractionation

The information that can be gained from structural analysis of the feedstock should preferably guide expected product formation upon its conversion by RCF. The aim here is to find distinct correlations between the detailed 2D HSQC NMR structural analysis and to link this to the products obtained from RCF. For this purpose, RCF of the lignocellulosic materials was performed using a commercially available Ru/C(5%) catalyst at published optimized parameters for lignin monomer release,[21,22] and the main released monomers such as 4-*n*-propylsyringol (S1) and -guaiacol (G1), and 4-*n*-propanolsyringol (S2) and -guaiacol (G2), as well as 4-*n*-ethylsyringol (S3) and -guaiacol (G3) were quantified (Figure 5a and Table S5). The relative ratio between G- and S-type monomers was generally higher than the value determined by 2D HSQC NMR spectroscopy. This was in particular observed for lignin with a higher amount of β-5 linkages, which is due to the presence of more β-5 and 5–5 type linkage-connected G units. Units with these C–C bonds are released as dimers or oligomers instead of monomers.

The highest monomer yield was achieved by RCF of birch wood, and pine showed the highest recalcitrance with a relative lower monomer yield. These overall monomer yields corresponded well to the relative proportion of β-O-4 linkage determined by 2D HSQC NMR spectroscopy for these lignins (WCW and REL samples), and the yield was consistent with previously reported values.[21,22] Walnut shell gave somewhat lower amounts of total monomers compared to reed than expected based on the β-O-4 linkage content, which is likely due to FA and *p*CA groups in reed (see below) combined with the higher H content in walnut shells linked to more stable C–C bonds. The latter could not be correlated to the amount of dimers and trimers in the product oil as determined by GPC analysis (Figure S20), and this effect might thus be minor compared to the effect of the monomers related to FA and *p*CA. The yield of methyl-3-(4-hydroxyl-3-methoxyphenyl) propionate (FMA) derived from methanol transesterification and double bond hydrogenation of FA was only observed in the product oil of reed, which was correlated to the presence of FA.

For the rest, a significant amount of products, in particular for reed, did not fall in the regular class of monomers with S and G aromatic ring substitution patterns. Therefore, we also carefully quantified the amounts of minor monomers. Monomers with H substitution patterns, such as 4-propylphenol (H1), 4-propylphenol (H2), and 4-ethylphenol (H3) were found, as well as products that are likely associated with *p*CA such as methyl 3-(4-hydroxyphenyl) propionate (PMA) and methyl 3-(4-hydroxycyclohexyl)propanoate (OHP) (Figure 5b, WCW samples). Walnut shell was shown to contain the highest amounts of H units by 2D HSQC NMR analysis, which also revealed the total monomer yield when only taking into account H1 and H2. This led us to conclude that H1 and H2 are the main products of H units that are part of the lignin chain originating from the *p*-coumaryl alcohol precursor in the lignin biosynthesis. The products from reed revealed overall the highest amounts of these minor phenolic compounds when other components such as H3, OHP, and PMA were considered (nearly 10% of the 35% total monomer yield). This indicates that these monomers are likely derived from *p*CA units that are abundant in reed. These results show that the nature of the H and its related units (*p*CA) significantly affect the products distribution from RCF of lignocellulosic biomass rich in such units, which can readily be deduced from 2D HSQC NMR analysis of the whole biomass. Nevertheless, the fact that the total amount of H1 and H2 in all the product oilswas less than 2%, means that lower amount of these products was produced than expected based on the 2D HSQC NMR results (up to 24% for walnut), indicating that their quantities in WCW samples are indeed likely significantly overestimated by 2D HSQC NMR spectroscopy.

Hydrogenolysis of isolated lignins

To further investigate the role of the H units and derivatives, hydrogenolysis of the different isolated lignins was performed (Figure 5c, d, REL and MWL). Overall, the amount of monomers was typically somewhat lower, but higher for REL than MWL, which overall showed a larger deviation from the reductive fractionation, in particular for birch. A similar distribution between S and G monomers was found that related well to the S/G ratio determined by 2D HSQC NMR spectroscopy. The only curious observation were the increased amounts of S1, G1 and H1 relative to S2, G2 and H2 (the M_W distribution also clearly revealed this difference, as shown in Figure S20). As the main difference between RCF and the hydrogenolysis of isolated lignin is the presence of saccharides, we performed control reactions where cellulose (Avicel ®PH-101) and xylan (birch) were added to REL samples followed by hydrogenolysis. Interestingly, the presence of birch xylan had a negative effect on the overall yield, which could be due to the presence of impurities introduced during its isolation. Nevertheless, the same trend in the product distribution was observed in terms of increased formation of S1, G1, and H1 relative to S2, G2, and H2 (Figure 6a). This led us to believe that the presence of carbohydrates significantly influences the catalyst selectivity leading to a different product distribution.

Regarding the minor units, also the distinct difference between reed and walnut shell is revealed. For walnut shell again the main products are H1 and H2, while reed samples contain more H3, OHP, and in particular PMA. The amount H3 decreased significantly for all samples going from RCF to hydrogenolysis of isolated lignins. H3 was highly suspected to be linked to *p*CA based on our initial analysis, even though the isolated lignins still seemed to contain *p*CA according to 2D HSQC NMR spectroscopy. So it seems that some other

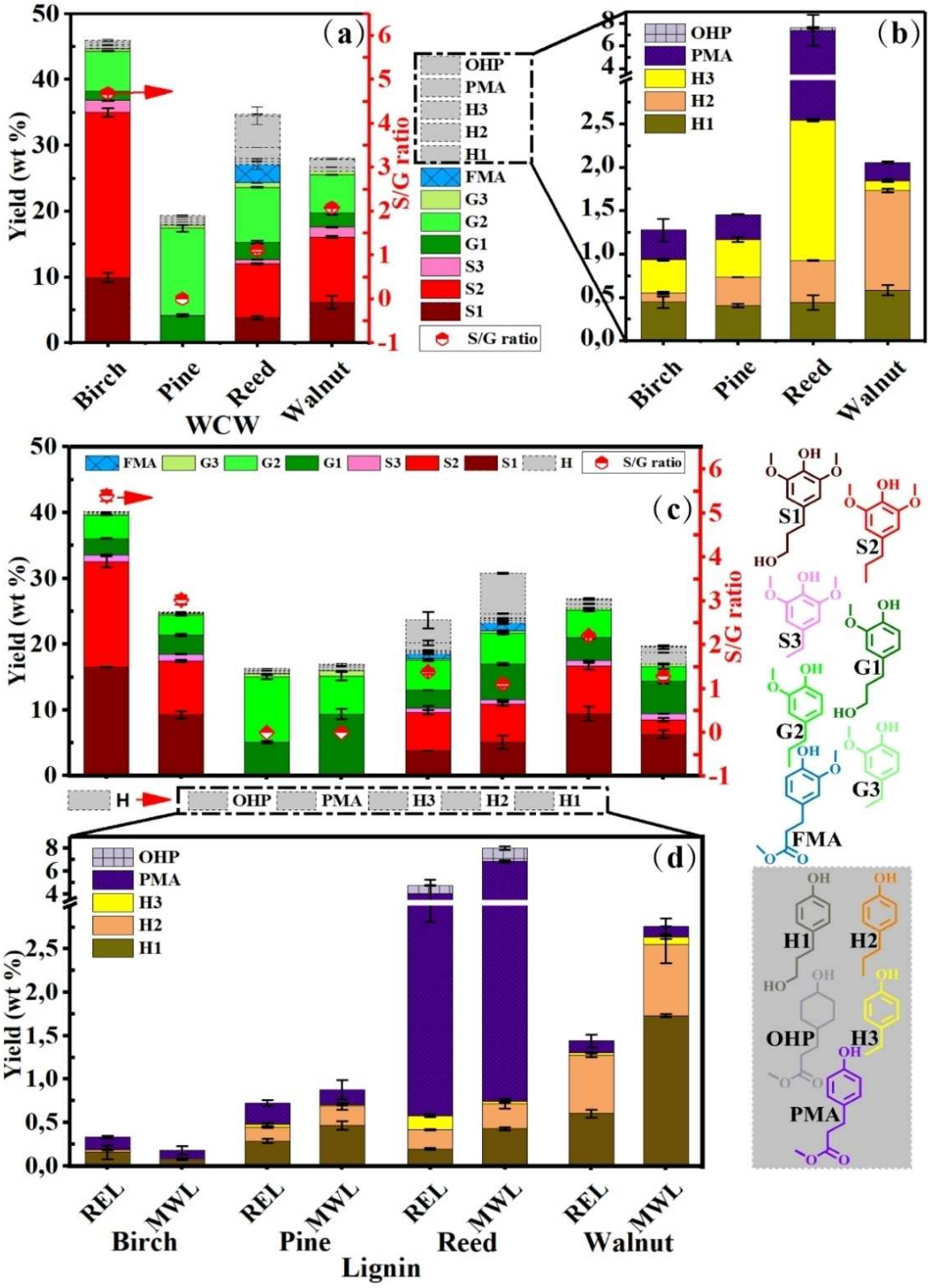

Figure 5. Monomers from RCF (WCW) and hydrogenolysis of REL, and MWL. The yieldswere corrected based on the carbohydrates analysis. (a) Data obtained from WCW materials. (b) H-related monomers from WCW samples. (c) Data from isolated lignin samples. (d) H-related monomers from isolated lignin samples. The chemical structures are colored and their yields have the same color in the figure. Monomer includes 4-(3-hydroxypropyl)-2,6-dimethoxyphenol (**S1**), 2,6-dimethoxy-4-propylphenol (**S2**), 4-ethyl-2,6-dimethoxyphenol (**S3**), 4-(3-hydroxypropyl)-2-methoxyphenol (**G1**), 2-methoxy-4-propylphenol (**G2**), 4-ethyl-2-methoxyphenol (**G3**), 4-(3-hydroxypropyl)phenol (**H1**), 4-propylphenol (**H2**), and 4-ethylphenol (**H3**). The products obtained from hydrogenation and methyl esterification include methyl 3-(4-hydroxyphenyl)propionate (PMA), methyl 3-(4-hydroxy-3-methoxyphenyl)propionate (FMA), and methyl 3-(4-hydroxycyclohexyl)propanoate (OHP). Reaction conditions: 250 mg biomass (50 mg for REL, 25 mg for MWL), 25 mg Ru/C (10 mg for MWL), 4 mL methanol, 250 °C, 3 h, and 60 bar H_2. The monomer yield of WCW materials was based on Klason lignin.

constituents or *p*CA linked to particular lignin or polysaccharide motifs in the raw biomass contribute to the production of H3.

Analysis of the dimer fractions

G units, but also H units, are expected to have more tendency to form C–C bonds such as 5,5 and β-5 linkages during biosynthesis, and thus their presence should lead to higher amounts of dimers, trimers, and oligomers. As mentioned above, GPC analysis of the oils did not really lead to any conclusive results (Figure S20), and therefore we further derivatized the oil obtained from hydrogenolysis of REL and MWL and performed a more in-depth GC-MS analysis (see Figures S24–S27 for the spectra of signals of identified dimers with the aid of previous dedicated publications[39,66]). Dimers derived from S and G units with linkage of β-β, β-5, and β-1 could be readily identified (see the Supporting Information Section S3). To correlate this analysis to the structure of the different lignins, a rough percentage of peak area of dimer correlated to different linkages was calculated (Tables S6 and S7). β-β and β-5 were the most readily linked to specific dimers and were thus most abundant, but their relative distribution between the biomass samples correlated excellently with the values obtained from 2D HSQC NMR analysis. As the H-derived monomer products are always lower than 2%, the identification of specific H-derived dimers was expected to be very challenging. Nevertheless, a significant attempt was made to find signals that corresponded to H units, and one H–G dimer derived from a β-β linkage could be assigned. This dimer had the highest relative abundance in the MWL_pine and MWL_walnut samples, which also had the highest combination of G and H units. Looking at the total amounts of dimers, it seems that in particular the pine-derived oils as well as the REL_walnut-derived oil showed significant amounts of dimers, which correlates well to the lower amounts of monomers. This fits the lower amounts of cleavable β-O-4 linkages in pine as well the significant presence of H and G units in these samples.

Monomers derived from *p*CA and FA

To gain further insight into the expected RCF product portfolio from *p*CA and FA, *p*-coumaric acid (*p*CCA), ferulic acid (FAA), and their methylated counterparts were converted under RCF conditions, and the products were analyzed (Figure 6b and Figure S21a). Both FAA and its methyl ester (FAMe) resulted in same product FME, which is the result of the side chain-hydrogenation (and esterification for FAA). No G3, G2, or G1 were observed in the reaction of FAA and FAMe, indicating that these components do not contribute to the main lignin hydrogenolysis products. However, FMA was found in the reed samples, and the relative amount (WCW > REL > MWL) matched the amounts of FA determined by 2D HSQC NMR spectroscopy of the different samples and also likely corresponded to associated hemicellulose residues, which were significantly lower in the isolated lignins. For *p*CCA and *p*CAMe a similar product (PMA) was found in 25% yield corresponding to the hydrogenation of the double bond and for *p*CCA methyl esterification. Moreover, the yield of PMA for WCW, REL, and MWL were similar to each other and all less than 5%, which correlated with the similar percentages of *p*CA quantified by 2D HSQC NMR spectroscopy in WCW, REL and MWL. But, the yield of PMA is much lower than might be expected based on the

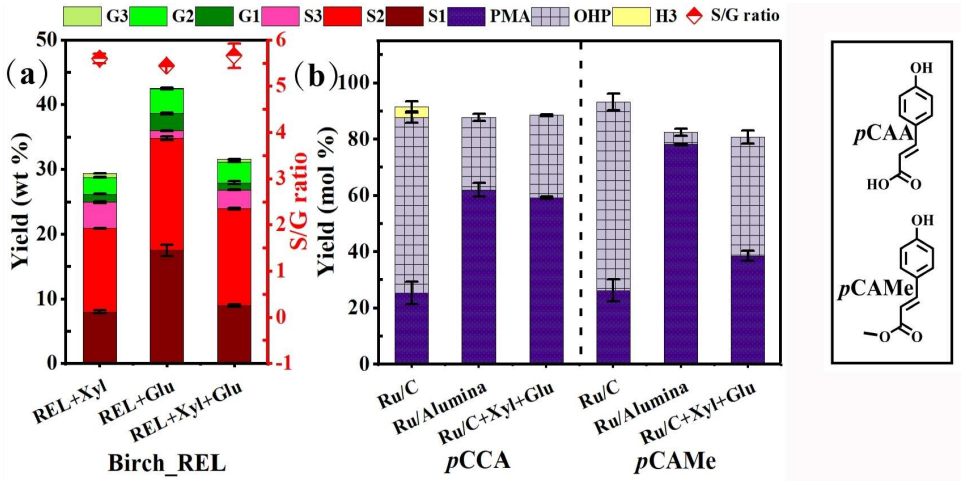

Figure 6. Monomers from hydrogenolysis of model compounds and the influence of polysaccharide addition for the monomer distribution. (a) Influence of polysaccharides on the monomer distribution obtained from Birch REL hydrogenolysis. Reaction conditions: "REL + Xyl": 50 mg Birch_REL, 60 mg xylan from birch, 25 mg Ru/C, 4 mL methanol, 250 °C, 3 h, 60 bar H_2; "REL + Glu": 50 mg Birch_REL,110 mg cellulose from cotton, 25 mg Ru/C, 4 mL methanol, 250 °C, 3 h, 60 bar H_2; "REL + Xyl + Glu": 50 mg Birch_REL,60 mg xylan from birch, 110 mg cellulose from cotton, 25 mg Ru/C, 4 mL methanol, 250 °C, 3 h, 60 bar H_2. The chemical structures are colored and their yields have the same corresponding color in the Figure 5 (b) Hydrogenolysis of model compounds with and without polysaccharide addition, including *p*-coumaric acid (*p*CCA) and methyl (*E*)-3-(4-hydroxyphenyl)acrylate (*p*CAMe). Reaction conditions: "Ru/C and Ru/Alumina": 20 mg start material, 10 mg Ru/C or Ru/Alumina, 4 mL methanol, 250 °C, 3 h, 60 bar H_2; "Ru/C + Xyl + Glu": 20 mg start material, 10 mg Ru/C or Ru/Alumina, 20 mg cellulose, 10 mg xylan, 4 mL methanol, 250 °C, 3 h, 60 bar H_2.

semi-quantification (more than 20% for all the reed samples), which further indicated the overestimation of these end groups by 2D HSQC NMR spectroscopy. Additionally, here also significant amounts (>65%) of the ring hydrogenation products (OHP) were found. These products were also formed in significant amounts in the reed samples in the order WCW < REL < MWL, matching the amount of carbohydrate residues in the samples. Indeed, control reactions with *p*CCA and *p*CAMe in the presence of cellulose and xylan showed also lower amounts of OHP, indicating that the formation of such over-hydrogenated products is inhibited by the presence of saccharides (Figure 6b). In total, through control experiments by the addition of carbohydrates to the isolated lignins and model compounds, it was found that the polysaccharide constituents inhibit dehydroxylation of the side chains of the aromatic monomers as well as over-hydrogenation of the aromatic rings.

Thus far, all products found from RCF could be traced back to individual structural units in the original lignins, however only the origin of H3 remained a bit of a mystery. For *p*CCA around 5% was degraded into H3 but none of the other model compound reactions gave any H3, which would be the result of a decarboxylation reaction. Changing the catalyst (Figure 6b), adding carbohydrates or changing to the corresponding ester *p*CAMe did suppress the formation of this small amount of H3. It was reported that alkoxide species play a very important role in surface interaction of compounds on catalysts and decarboxylation reactions,[67,68] and thus the free acid might still be partly responsible for the formation of H3. In addition, hemicellulose constituents of *p*CA with free carboxylic acid end group have been reported[69] but under reaction conditions are likely quickly esterified as the model compound reactions revealed. We further used a hemicellulose extracted from mixed grasses and rich in *p*CA (Figure S22) for an additional control reaction. The main products were derived from *p*CA and FA, and only trace amounts of H monomers were monitored (Figures S21c and S23). Finally, the stability of H1, H2, and H3 in this reductive treatment was investigated (Figure S21b), revealing trace amounts of H3 that was produced from reductive treatment of H1, which indicated that H3 could also be formed by further reactivity of these components in solution, but the difference in yield of H3 from the different biomasses could not fully traced back to the specific structures of the original biomass samples, and it is likely that an unidentified effect or biomass constituent also plays a role in the formation of H3.

Conclusion

Overall, in this study, lignins in four representative biomasses were comparable evaluated by whole cell wall (WCW), residual enzyme lignin (REL), and milled wood lignin (MWL), and the reliability and concordance of lignin analyses based on the three protocols was discussed. Gel-state 2D heteronuclear single quantum coherence (HSQC) NMR spectroscopy provided detailed structural information of the WCW after milling, but the overestimation of end group was an issue. REL was more representative than MWL to reveal the integrated structure of lignin in terms of larger molecular weight and much detail in linking units. Comparing the 2D HSQC NMR analyses, relatively big differences were observed for birch and walnut shell in terms proportion of units and linkage content, with the WCW and REL providing more similar results. When relating these analyses to monomer yield and distribution obtained from reductive catalytic fractionation (RCF) led to a clear correlation between monomer distribution and main linkages and aromatic unit constituents of the original lignin component of the biomass as determined by 2D HSQC NMR samples. Overall, comparing the monomer yield and similar distribution with that of WCW indicated that the product of REL hydrogenolysis is more representative than that of MWL to reveal the actual behavior of lignin during reductive fractionation. One disadvantage of REL analysis is that ferulic acid units linked to hemicellulose are removed, which will end up in the phenolic product mixture and thus contribute to the total monomer yield. The presence of polysaccharide constituents such as xylan and cellulose significantly influences the aromatic monomer selectivity and inhibits over-hydrogenation of the aromatic ring as well as dehydroxylation to give more propanol-substituted aromatic monomers. Furthermore, the RCF products from minor units significantly impacted product distributions. For instance, a higher amount of H units predominantly led to increasing amount of H1 and H2 especially for the reed and walnut shell biomass. In particular, *p*-coumaric acid units in reed contributed nearly 10% of the 35% of the monomeric product mixture. In-depth analysis of the monomer distribution derived from minor units indeed enhanced understanding of their original state and structure in lignin and biomass. The relative quantities of these units were more readily accurately quantified by 2D HSQC NMR spectroscopy of REL samples compared to ge-state 2D HSQC NMR of the WCW due to overestimation of these pendant units. In total, this study shows how different analyses of the lignin structure of the original biomass can provide good prediction to the obtained monomer portfolio from RCF of different biomass and the effects of minor units and carbohydrate impurities. This information can guide studies on the viability of "lignin-first" related biorefinery efforts.

Experimental Section

General remarks

All the chemicals were used as received and purchased from Sigma-Aldrich or Fluorochem unless otherwise noted. Birch wood, pine, reed, and walnut shells were picked up from local sources. The catalyst used for RCF/hydrogenolysis was 5% Ru on carbon and aluminum oxide (Sigma). *p*-Coumuric acid (*p*CCA), ferulic acid (FAA), xylan from birch, and Avicel®PH-101 cellulose from cotton were also purchased from Sigma-Aldrich. Solvents were supplied by Fisher Scientific. Some standard chemicals including 4-(3-hydroxypropyl)-2,6-dimethoxyphenol (S1), 2,6-dimethoxy-4-propylphenol (S2), 4-ethyl-2,6-dimethoxyphenol (S3), methyl 3-(4-hydroxy-3-methoxyphenyl)propanoate (FMA), methyl (*E*)-3-(4-hydroxy-3-methoxyphenyl)acrylate (FAMe), methyl 3-(4-hydroxyphenyl)propanoate (PMA), hydroxycyclohexyl)propanoate (OHP), and methyl (*E*)-3-(4-hydroxyphenyl)acrylate (*p*CAMe) were synthesized and isolated for

this study, (S1.5, Figures S1–11). More detailed information on the synthetic and analytical procedures can be found in the Supporting Information.

Lignocellulose sample pretreatment

Biomass samples were cut into small sections and grounded in a Wiley mill with a 20-mesh screen and extracted with 1:2 (*v*/*v*) ethanol/benzene for 8 h in a Soxhlet apparatus. After volatilizing the solvents, the extract-free samples were dried at 65 °C for 16 h and stored in a valve bag before use. Ball milling was conducted in a planetary ball milling instrument (Fritsch GmbH, Idar-Oberstein, Germany) in the presence of 250 mL ZrO_2 jar and balls (5, 15 mm, 10, 5 mm) and a program with 450 rpm rotation, 10 min milling, and 15 min pausing were used for all the samples, and the time displayed throughout the manuscript only represents the active milling time, excluding the time for pauses in between. The 50 mM acetate buffer was prepared by directly dissolving the pre/calculated sodium acetate and adjusting the pH to 5.5 by adding acetic acid. Tetracycline chloride was added into the buffer to make a concentration of 0.8 mM based on the volume of the buffer to inhibit the growth of bacteria. All the enzymatic hydrolysis reactions were conducted at 50 °C in a VWR incubating orbital shaker (Model 3500L) at 250 rpm for 72 h with a solid/liquid ratio of 25.

Whole cell wall sample preparation and NMR experiments

The sample for WCW analysis was prepared according to a published procedure with minor modifications.[46] Ball milling for walnut shells started from around 30 g biomass, and 5 g sample was taken from the jar after milling 6, 12, and 24 h, and birch, pine, and reed sample were milled 24 h from a 10 g scale, and the swelling was conducted by submerging 80 mg milled biomass sample in premixed 0.7 mL DMSO-d_6/pyridine-d_5 solvent and sonicated for 1–5 h until a gel-state sample appeared.

Residual enzyme lignin isolation

The REL was isolated by following our previous publication.[47] 10 g biomass with 6 h ball-milled sample was used for the first enzymatic hydrolysis, after the treatment, the solid product was separated by centrifugation and freeze-dried using a lyophilizer (ALPHA 2-4 LD, Appropriate Technical Resources), and then the dried residue was further milled for 6 h before the second enzymatic hydrolysis treatment. The enzyme (Ctec2, Novozymes) loading for hydrolysis is 0.5 mL (g substrate)$^{-1}$. Accordingly, the solids obtained from the second treatment were noted as samples with a prefix of REL.

Extraction of milled wood lignin

The milled wood lignin was extracted by following published steps.[48] 20 g wood powder obtained from 6 h ball-milling described above was suspended in 400 mL dioxane/water (*v*/*v*, 96:4) and stirred for 24 h under dark, and residue was collected by centrifugation and further extracted by fresh solvent for another 24 h. The liquid was combined and condensed to approximately 30 mL, and further precipitated in 3 volume times 96% ethanol. After separation with centrifugation, the ethanol phase was concentrated to around 30 mL (this step was repeated) and the lignin was precipitated in 10 volume times acid water (pH = 2). The lignin was isolated by filtration and further washed by acid water and freeze dried.

Reductive catalytic fractionation/hydrogenolysis

RCF/hydrogenolysis was performed by using optimized parameters from a published paper with minor modification,[21] with a Ru/C catalysis in methanol. For each reaction, a 10 mL homemade batch reactor was loaded with 250 mg of lignocellulose or 50 mg isolated lignin (for MWL, 20 mg), 4 mL methanol (for MWL, 2 mL methanol), 25 mg of 5 wt.% Ru/C (for MWL, 10 mg of Ru/C) and a magnetic stirring bar. The reactor was closed, and 60 bar H_2 was charged at room temperature before heating. After 30 minutes, once the pressure of H_2 constantly keep at 60 bar, the reactor was put into a preheated oil bath with a temperature of 250 °C at a 300 rpm stirring. 3 h later, the reaction was terminated by washing the reactor with cooling tap water. 4 mL methanol (for MWL, 2 mL) with a concentration of 0.004 mmol mL^{-1} octadecane was added to the reactor before filtration for quantitation and dilution. 1 mL was transferred to a GC vial and filtered using a 0.45 μm polytetrafluoroethylene (PTFE) filter before injection into GC-flame ionization detector (FID). GC-FID used for the quantitation of monomers was an Agilent 8860. The following operating conditions were used: injection volume: 1 μL, injection temperature: 280 °C, column temperature program: 40 °C (5 min),10 °C min^{-1} to 320 °C, 320 °C (5 min), detection temperature 320 °C. The calibration was built by corresponding standard monomers with octadecane as reference (see S1.6), and curves were attached in the Supporting Information (Figure S19).

Acknowledgements

Z.W. acknowledges the China Scholarship Council for funding (grant number 201706300138). The authors would like to acknowledge Johanna H. L. Kaelen and Lambert J. Deuss for providing the walnut shells, A. Bakker, Harkstede for providing birch wood, and Prof. Gert Jan Euverink for providing reed for lignin isolation, as well as Slavador Bertran Llorens for providing a sample of hemicellulose from extracted from mixed grasses, and Xianyuan Wu for the synthesis of 4-(3-hydroxypropyl)-2,6-dimethoxphenol. Analytical support was provided by Leon Rohrbach and Johan Kemmink.

Conflict of Interest

The authors declare no conflict of interest.

Keywords: 2D HSQC NMR · biomass · lignocellulose · residual enzyme lignin · reductive fractionation

[1] J.-F. Bastin, Y. Finegold, C. Garcia, D. Mollicone, M. Rezende, D. Routh, C. M. Zohner, T. W. Crowther, *Science* **2019**, *365*, 76–79.
[2] J. E. Holladay, J. F. White, J. J. Bozell, D. Johnson, *Top Value-Added Chemicals from Biomass-Volume II – Results of Screening for Potential Candidates from Biorefinery Lignin*, Pacific Northwest National Lab. (PNNL), Richland, WA (United States), **2007**.
[3] A. J. Ragauskas, G. T. Beckham, M. J. Biddy, R. Chandra, F. Chen, M. F. Davis, B. H. Davison, R. A. Dixon, P. Gilna, M. Keller, P. Langan, A. K. Naskar, J. N. Saddler, T. J. Tschaplinski, G. A. Tuskan, C. E. Wyman, *Science* **2014**, *344*, 1246843.
[4] P. Rippert, J. Puyaubert, D. Grisollet, L. Derrier, M. Matringe, *Plant Physiol.* **2009**, *149*, 1251–1260.
[5] J. Ralph, G. Brunow, P. J. Harris, R. A. Dixon, P. F. Schatz, W. Boerjan, *Recent Adv. Polyphen. Res.* **2008**, *1*, 36–66.

[6] R. Vanholme, B. Demedts, K. Morreel, J. Ralph, W. Boerjan, *Plant Physiol.* **2010**, *153*, 895–905.
[7] S. Quideau, J. Ralph, *J. Chem. Soc. Perkin Trans. 1* **1997**, *16*, 2351–2358.
[8] W. Lan, F. Lu, M. Regner, Y. Zhu, J. Rencoret, S. A. Ralph, U. I. Zakai, K. Morreel, W. Boerjan, J. Ralph, *Plant Physiol.* **2015**, *167*, 1284–1295.
[9] L. Zhang, G. Gellerstedt, J. Ralph, F. Lu, *J. Wood Chem. Technol.* **2006**, *26*, 65–79.
[10] S. D. Mansfield, H. Kim, F. Lu, J. Ralph, *Nat. Protoc.* **2012**, *7*, 1579–1589.
[11] J. Ralph, P. F. Schatz, F. Lu, H. Kim, T. Akiyama, S. F. Nelsen, *Quinone Methides* **2009**, *1*, 385–420.
[12] A. Eudes, A. George, P. Mukerjee, J. S. Kim, B. Pollet, P. I. Benke, F. Yang, P. Mitra, L. Sun, Ö. P. Çetinkol, *Plant Biotechnol. J.* **2012**, *10*, 609–620.
[13] C. G. Wilkerson, S. D. Mansfield, F. Lu, S. Withers, J.-Y. Park, S. D. Karlen, E. Gonzales-Vigil, D. Padmakshan, F. Unda, J. Rencoret, *Science* **2014**, *344*, 90–93.
[14] J. Chen, X. Fan, L. Zhang, X. Chen, S. Sun, R. Sun, *ChemSusChem* **2020**, *13*, 4356–4366.
[15] Z. Sun, B. Fridrich, A. De Santi, S. Elangovan, K. Barta, *Chem. Rev.* **2018**, *118*, 614–678.
[16] J. G. Linger, D. R. Vardon, M. T. Guarnieri, E. M. Karp, G. B. Hunsinger, M. A. Franden, C. W. Johnson, G. Chupka, T. J. Strathmann, P. T. Pienkos, *Proc. Natl. Acad. Sci. USA* **2014**, *111*, 12013–12018.
[17] C. Li, X. Zhao, A. Wang, G. W. Huber, T. Zhang, *Chem. Rev.* **2015**, *115*, 11559–11624.
[18] C. Sáiz-Jiménez, J. W. De Leeuw, *Org. Geochem.* **1986**, *10*, 869–876.
[19] C. S. Lancefield, O. S. Ojo, F. Tran, N. J. Westwood, *Angew. Chem. Int. Ed.* **2015**, *54*, 258–262; *Angew. Chem.* **2015**, *127*, 260–264.
[20] A. Rahimi, A. Azarpira, H. Kim, J. Ralph, S. S. Stahl, *J. Am. Chem. Soc.* **2013**, *135*, 6415–6418.
[21] S. Van den Bosch, W. Schutyser, R. Vanholme, T. Driessen, S.-F. Koelewijn, T. Renders, B. De Meester, W. J. J. Huijgen, W. Dehaen, C. M. Courtin, *Energy Environ. Sci.* **2015**, *8*, 1748–1763.
[22] Y. Liao, S.-F. Koelewijn, G. Van den Bossche, J. Van Aelst, S. Van den Bosch, T. Renders, K. Navare, T. Nicolaï, K. Van Aelst, M. Maesen, *Science* **2020**, *367*, 1385–1390.
[23] E. Cooreman, T. Vangeel, K. Van Aelst, J. Van Aelst, J. Lauwaert, J. W. Thybaut, S. Van Den Bosch, B. F. Sels, *Ind. Eng. Chem. Res.* **2020**, *59*, 17035–17045.
[24] P. Sudarsanam, D. Ruijten, Y. Liao, T. Renders, S.-F. Koelewijn, B. F. Sels, *Trends Chem.* **2020**, *2*, 898–913.
[25] W. Schutyser, T. Renders, S. Van Den Bosch, S. F. Koelewijn, G. T. Beckham, B. F. Sels, *Chem. Soc. Rev.* **2018**, *47*, 852–908.
[26] H. Zhang, S. Fu, X. Du, Y. Deng, *ChemSusChem* **2021**, *14*, 2268–2294.
[27] X. Ouyang, X. Huang, M. D. Boot, E. J. M. Hensen, *ChemSusChem* **2020**, *13*, 1705–1709.
[28] S. Wang, W. Gao, H. Li, L. Xiao, R. Sun, G. Song, *ChemSusChem* **2018**, *11*, 2114–2123.
[29] X. Gong, J. Sun, X. Xu, B. Wang, H. Li, F. Peng, *Bioresour. Technol.* **2021**, *333*, 124977.
[30] C. Jose, A. Gutiérrez, I. M. Rodríguez, D. Ibarra, A. T. Martinez, *J. Anal. Appl. Pyrolysis* **2007**, *79*, 39–46.
[31] C. G. Boeriu, D. Bravo, R. J. A. Gosselink, J. E. G. van Dam, *Ind. Crops Prod.* **2004**, *20*, 205–218.
[32] X. Kang, A. Kirui, M. C. Dickwella Widanage, F. Mentink-Vigier, D. J. Cosgrove, T. Wang, *Nat. Commun.* **2019**, *10*, 1–9.
[33] C. L. Chen in *Methods Lignin Chemistry*, Springer, **1992**, pp. 301–321.
[34] G. Van Erven, R. de Visser, D. W. H. Merkx, W. Strolenberg, P. de Gijsel, H. Gruppen, M. A. Kabel, *Anal. Chem.* **2017**, *89*, 10907–10916.
[35] F. Lu, J. Ralph, *J. Agric. Food Chem.* **1997**, *45*, 4655–4660.
[36] F. Lu, J. Ralph, *J. Agric. Food Chem.* **1997**, *45*, 2590–2592.
[37] J. H. Grabber, S. Quideau, J. Ralph, *Phytochemistry* **1996**, *43*, 1189–1194.
[38] Y. Li, S. D. Karlen, B. Demir, H. Kim, J. Luterbacher, J. A. Dumesic, S. S. Stahl, J. Ralph, *ChemSusChem* **2020**, *13*, 4487–4494.
[39] E. M. Anderson, M. L. Stone, R. Katahira, M. Reed, W. Muchero, K. J. Ramirez, G. T. Beckham, Y. Román-Leshkov, *Nat. Commun.* **2019**, *10*, 1–10.
[40] J. Ralph, J. M. Marita, S. A. Ralph, R. D. Hatfield, F. Lu, R. M. Ede, J. Peng, L. L. Landucci, *Adv. Lignocellul. Charact.* Atlanta, Ga. TAPPI Press. c1999. p. 55–108 ill. **1999**.
[41] J. L. Wen, S. L. Sun, B. L. Xue, R. C. Sun, *Materials* **2013**, *6*, 359–391.
[42] C. Heitner, D. Dimmel, J. Schmidt, *Lignin and Lignans: Advances in Chemistry*, CRC Press, **2016**.
[43] H. Chang, E. B. Cowling, W. Brown, *Holzforschung* **1975**, *29*, 153–159.
[44] H. Kim, D. Padmakshan, Y. Li, J. Rencoret, R. D. Hatfield, J. Ralph, *Biomacromolecules* **2017**, *18*, 4184–4195.
[45] A. Guerra, I. Filpponen, L. A. Lucia, D. S. Argyropoulos, *J. Agric. Food Chem.* **2006**, *54*, 9696–9705.
[46] K. M. Holtman, H. Chang, J. F. Kadla, *J. Wood Chem. Technol.* **2007**, *27*, 179–200.
[47] T. Ikeda, K. Holtman, J. F. Kadla, H. M. Chang, H. Jameel, *J. Agric. Food Chem.* **2002**, *50*, 129–135.
[48] H. Kim, J. Ralph, *Org. Biomol. Chem.* **2010**, *8*, 576–591.
[49] Z. Wang, X. Zhu, P. J. Deuss, *Ind. Crops Prod.* **2021**, *167*, 113493.
[50] J. L. Wen, S. L. Sun, B. L. Xue, R. C. Sun, *Holzforschung* **2013**, *67*, 613–627.
[51] FAO, FAOSTAT Data, Food and Agriculture Organization (http://www.fao.org/faostat/en/#data/QC) **2016**.
[52] S. A. Ralph, J. Ralph, L. Landucci, L. L. Landucci, US For. Prod. Lab., Madison, WI (http://ars.usda.gov/Services/docs.htm) **2004**.
[53] H. Kim, J. Ralph, *RSC Adv.* **2014**, *4*, 7549–7560.
[54] J. Ralph, R. D. Hatfield, S. Quideau, R. F. Helm, J. H. Grabber, H.-J. G. Jung, *J. Am. Chem. Soc.* **1994**, *116*, 9448–9456.
[55] J. Ralph, C. Lapierre, W. Boerjan, *Curr. Opin. Biotechnol.* **2019**, *56*, 240–249.
[56] F. Yue, F. Lu, S. Ralph, J. Ralph, *Biomacromolecules* **2016**, *17*, 1909–1920.
[57] P. Karhunen, P. Rummakko, J. Sipilä, G. Brunow, I. Kilpeläinen, *Tetrahedron Lett.* **1995**, *36*, 169–170.
[58] M. Sette, R. Wechselberger, C. Crestini, *Chem. Eur. J.* **2011**, *17*, 9529–9535.
[59] D. S. Zijlstra, C. W. Lahive, C. A. Analbers, M. B. Figueirêdo, Z. Wang, C. S. Lancefield, P. J. Deuss, *ACS Sustainable Chem. Eng.* **2020**, *8*, 5119–5131.
[60] P. J. Deuss, M. Scott, F. Tran, N. J. Westwood, J. G. De Vries, K. Barta, *J. Am. Chem. Soc.* **2015**, *137*, 7456–7467.
[61] R. Vanholme, B. De Meester, J. Ralph, W. Boerjan, *Curr. Opin. Biotechnol.* **2019**, *56*, 230–239.
[62] T. Özben, *Free Radicals, Oxidative Stress, and Antioxidants: Pathological and Physiological Significance*, Springer Science & Business Media, **2013**.
[63] S. D. Karlen, C. Zhang, M. L. Peck, R. A. Smith, D. Padmakshan, K. E. Helmich, H. C. A. Free, S. Lee, B. G. Smith, F. Lu, J. C. Sedbrook, R. Sibout, J. H. Grabber, T. M. Runge, K. S. Mysore, P. J. Harris, L. E. Bartley, J. Ralph, *Sci. Adv.* **2016**, *2*, 1–10.
[64] F. Lu, J. Ralph, *Org. Biomol. Chem.* **2008**, *6*, 3681–3694.
[65] F. Lu, J. Ralph in *Proc. 13th Int. Symp. Wood, Fiber, Pulping Chem.* **2005**, 16–19.
[66] S. Van den Bosch, W. Schutyser, S.-F. Koelewijn, T. Renders, C. M. Courtin, B. F. Sels, *Chem. Commun.* **2015**, *51*, 13158–13161.
[67] G. Calvaruso, J. A. Burak, M. T. Clough, M. Kennema, F. Meemken, R. Rinaldi, *ChemCatChem* **2017**, *9*, 2627–2632.
[68] J. Le Nôtre, S. C. M. Witte-van Dijk, J. van Haveren, E. L. Scott, J. P. M. Sanders, *ChemSusChem* **2014**, *7*, 2712–2720.
[69] K. Pei, J. Ou, J. Huang, S. Ou, *J. Sci. Food Agric.* **2016**, *96*, 2952–2962.

Manuscript received: July 19, 2021
Revised manuscript received: August 13, 2021
Accepted manuscript online: August 16, 2021
Version of record online: September 20, 2021